STUDIA UNIVERSITATIS BABEŞ-BOLYAI, CHEMIA, L, 2, 2005

NAMING POLYHEX TUBULAR OBJECTS ORIGINATING IN SQUARE TILED LATTICES

MIRCEA V. DIUDEA and SIMONA S. CIGHER

Faculty of Chemistry and Chemical Engineering, Babeş-Bolyai University, 400028 Cluj, Romania

ABSTRACT. Tiling of a tubular nanostructure can be modified, from the tetragonal (4,4) to hexagonal (6,3) by cutting procedures. As implemented in the Torus software program, these provide tubular/toroidal objects of various size, embedding and covering. Naming polyhex tubular objects is given both in Diudea and Hamada terms. Topological description by α-spiral code was adapted for polyhex tubular and toroidal nets.

1.INTRODUCTION

Covering a local planar surface by various polygonal or curved regions is an ancient human activity. It occurred in house building, particularly in floor, windows and ceiling decoration. There were well known three regular Platonic tessellations: (4,4), (6,3) and (3,6). The Greek and Roman mosaics were very appreciated in this respect.

Covering is nowadays a mathematically founded science.[1] It makes use of the Graph and Set Theory and often inspires from the Arts and Architecture.

Covering transformation is one of the ways in understanding chemical reactions occurring in nanostructures.[2-4]

Among the carbon allotropes, intensively studied in the last decade,[5-9] the only orientable closed surface *S* entirely coverable by a benzenoid lattice is the torus. A polyhedral cage obeys the Euler theorem[10].

$$N - E + F = 2(1 - g) \quad (1)$$

where *N, E, F,* and *g* are respectively the number of vertices, edges, faces, and genus – zero for the sphere and unity, in case of the torus.

The article is organised as follows. The second section introduces to some cutting procedures performed on the chessboard tessellation embedded in torus and cylinder. A third section deals with the perfect Clar structures and the perfect Corannulenic systems. The last two sections provide conclusions and references.

2.CUTTING PROCEDURES ON (4,4) TESSELLATION

Embedding[5] (*i.e*., drawing of a graph on a (closed) surface with no crossing lines) of the hexagonal trivalent (6,3) net (cf. the Schäfli notation) in the torus or the cylinder is achieved mainly by the well-known graphite zone-folding.[11,13,14,19-21]

The method finds an equivalent planar parallelogram, tiled with the graphitic polyhex lattice. When two opposite edges are identified, a tube is formed, which is completely defined by two integer parameters (*k*,*l*), according to Hamada *et al*.[22] The two parameters quantify (in terms of the primitive lattice vectors of graphene) the *chiral* vector *R* on which the tube is rolled up. In case: *armchair* A, (*k*,*k*) and *zigzag* Z, (*k*,0), the tube is achiral. The translation vector *T* follows the tube axis and is orthogonal to *R*

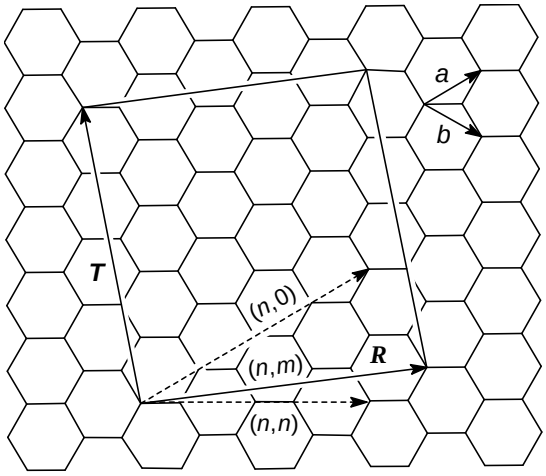

Figure 1. The rolled up area delimited by *T* and *R* corresponds to the *repeat unit* of an (*n*,*m*) *chiral tube*, ((3,2) in Figure; the achiral limit cases (n,0) and (n,n) are (4,0) and (2,2), respectively.

When the two remaining edges are further identified (*cf*., the *translation* or twisting vector *T*) the torus thus obtained is completely defined by four integers (*e.g*., (*k,l,p,q*)), reducible to three parameters, according to Kirby *et a*l.[12,14]

An alternative to the parallelogram procedure uses the topological coordinates, extracted from the adjacency matrix eigenvectors.[15-18]

2.1. Basic Polyhex Constructions

Our construction starts with embedding of the tetragonal (4,4) net on either the cylinder or torus.[23-28]

A cylindrical surface is covered by a square net as follows:

- take the cross section of a *c* -fold polygon and move it along the cylinder axis;
- join the *n* subsequent images of the polygon, to form a tube.

The parameters are calculated by the cylindrical coordinates as:

$$P(x, y, z) \tag{2}$$
$$x = r\cos\theta$$
$$y = r\sin\theta$$
$$z = z$$
$$\theta_i = \frac{2\pi}{c} i \quad ; \quad i = 0,...,c-1$$
$$z_i = \frac{z}{n} i \quad ; \quad i = 0,...,n-1$$

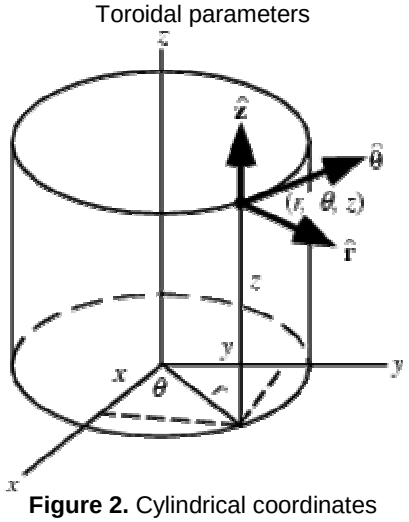

Figure 2. Cylindrical coordinates

The embedding of the (4,4) net on the torus is made by circulating a *c*-fold cycle, circumscribed to the toroidal tube cross-section of radius *r*, around the large hollow of the torus, of radius $R > r$ (Figure 3). Its subsequent *n images*, equally spaced and joined with edges, point by point, form a polyhedral torus tiled by a tetragonal pattern. The position of each of the *n* images of the "circulant" around the central hollow is characterized by angle θ while angle φ locates the *c* points across the tube. In all, *c* x *n* points are generated. The parameters *R* and *r* are not directly involved in the topological characterization of the lattice.

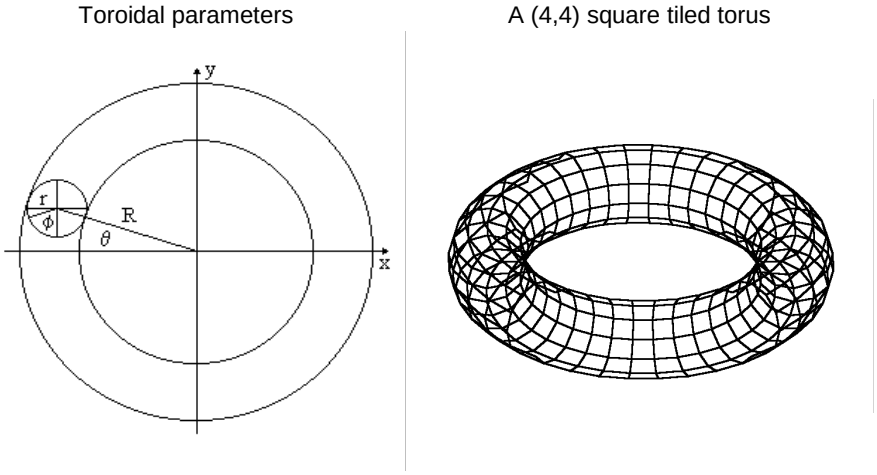

Figure 3. Embedding of the (4,4) net in the torus.

The parameters are calculated by the following formulas:

$$P(x, y, z): \tag{3}$$

$$x = \cos(\theta)(R + r\cos\varphi)$$

$$y = \sin(\theta)(R + r\cos\varphi)$$

$$z = r\sin\varphi$$

$$\theta_i = \frac{2\pi}{n} i \quad ; \quad i = 0,...,n-1$$

$$\varphi_j = \frac{2\pi}{c} j \quad ; \quad j = 0,...,c-1$$

The tetragonal objects thus obtained are named by a string specifying the tiling and dimensions of the net: (4,4)[*c*,*n*] (for tubes, Tu is added in the front of), with the (integer) parameters in the square brackets being the number of atoms in the tube cross-section and the number of cross-sections around the torus (or along the tube), respectively. The objects consist of $c \times n$ vertices, $c \times n$ squares and $4 \times c \times n/2$ edges, 4 being the vertex degree of the net (which is a regular graph). This covering appears in some metal clusters and silicon nanotubes.[29,30]

Next, the tetragonal (4,4) net is modified to give, most often, a hexagonal (6,3) net or other patterns, of chemical interest. Several cutting procedures we have developed in this respect.[24-28,31,32]

A cutting operation consists of deleting appropriate edges in a tetragonal (4,4) lattice in order to produce some larger polygonal faces. By deleting each second *horizontal* edge and alternating edges and cuts in each second row it results in a standard (6,3)H/Z pattern (Figure 4,a). A *vertical* action of the above algorithm leads to a standard (6,3)V/A pattern (Figure 4,b). The specifications Z (zigzag) and A (armchair) come from the shape of the tube cross-section.

(a) (6,3)H/Z pattern (b) (6,3)V/A pattern

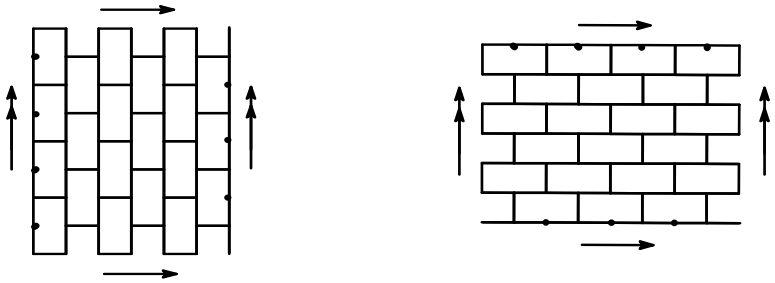

Figure 4. The (6,3) covering by H- (a) and V- (b) cutting of the (4,4) net. Note that each hexagon consumes exactly two squares of the (4,4) lattice.

By construction, the number of hexagons in the H/Z-objects is half the number of squares on dimension *c* while, in V/A-objects, the reduced number of hexagons appears on dimension *n*. Thus, (6,3)Z[2*c*,*n*] has the same number of hexes as its embedding isomer (6,3)A[*c*,2*n*]. Recall that, the above cutting procedure leaves unchanged the number of vertices in the original (4,4) lattice.

After optimizing, *e.g*., by a Molecular Mechanics procedure, (6,3) lattices appear like in Figure 5.

(a) Tu(6,3)A[12,12]; N = 144 (b) (6,3)H/Z[12,50]; N = 600

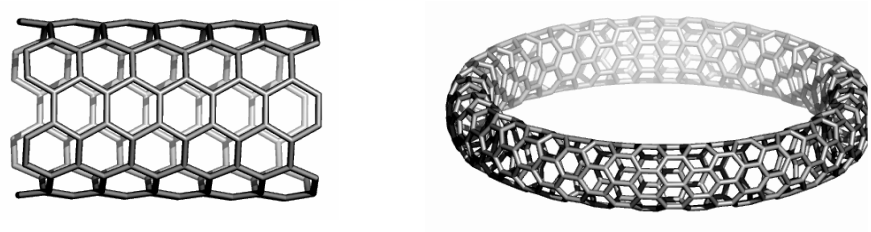

Figure 5. The (6,3) covering in the cylindrical and toroidal embedding, respectively.

2.2. Twisted/Chiral Polyhex Structures

Twisted, chiral, patterns can be generated by the following two procedures: (1) horizontal twisting of a layer of connections (Figure 6a) and (2) vertical twisting (offset) of the end connections (not shown). In cylindrical embedding, only one twisting type (namely the one parallel to the cylinder generator) will work, because of the open ends. Edge cutting is further needed to change squares into hexagons (Figure 6b). Twisting an even number of layers is needed to obtain a hexagonal net. The type of cutting will dictate the type of embedding and, ultimately, the shape of objects.

(a) (4,4) net (b) (6,3) net

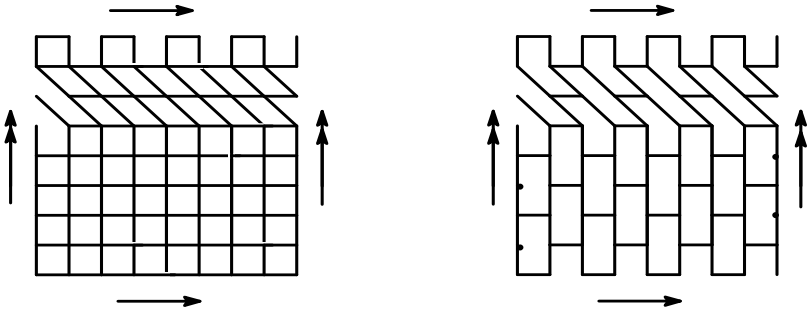

Figure 6. Twisted (4,4) pattern (a) and its (6,3) derivative (b).

The twisting parameter *t* takes integer values in the range [0,*c*]. It is just the deviation (in number of hexagons) of the chiral (*i.e*., rolling-up) vector to the zigzag line, in the graphite sheet representation.[11-14,20,21]

In case of tubes, Tu(6,3)HH*t*[*c*,*n*], the number of atoms on the *c*-dimension increases as *t* increases, concomitant with the shortening of *n*-dimension (in general, non-integer values, having a statistical meaning).[33] The twisting preserves the type of net (Z, in this case) and the total number of hexagons as well (*i*.*e*., (*c*/2) × (*n*-1)), the same as in the non-twisted tube). Correspondingly, the number of "zigzags" (*i*.*e*., the number of end-hexagons) increases, from *c*/2 up to twice the initial value. The final object will be Tu(6,3)HH*c*[*c*,*n*] = Tu(6,3)Z[2*c*,*n*/2]. Note that diameter doubling of single walled nanotubes has been observed experimentally [34,35] and termed "tube coalescence".

In case of Tu(6,3)HV*t*[*c*,*n*], the twisting keeps the *c*, *n* dimensions but stepwise adds the Z-character (*i*.*e*., adds zigzag hexagons), finishing in a pure Z-net, particularly Tu(6,3)Z[2*c*,*n*/2]. The crenel and zigzag tips coexist, as can be seen from Figure 7 (the right column). The two embeddings, HH and HV can be named by two integer parameters, according to Hamada *et al*.[22]

Clearly, both local covering and embedding (*i*.*e*., global covering) contribute to the structural (and electronic) properties of the tubular nanostructures.

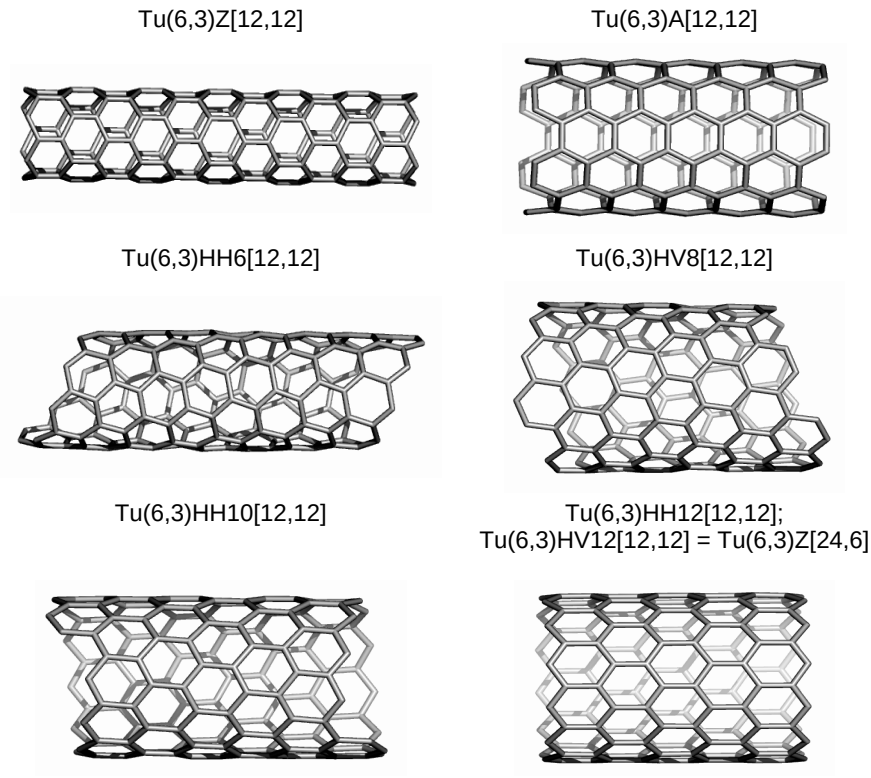

Figure 7. Nanotube twisting; diameter doubling at *t* = *c* is evident by comparing the top left corner tube with the bottom right one.

Correspondence between the name of polyhex tubes in our approach and the two integer parameter (*k*,*l*) notation is given below:

$$\mathrm{TUH/Z}[c,n]: \quad c=2k; \quad t=0; \quad \mathrm{Z}(c/2,0) \tag{4}$$

$$\mathrm{TUHH}t[c,n]: \quad c=2k+l; \quad t=|c-2k|; \quad k=(c-t)/2; \quad l=t \tag{5}$$

$$\mathrm{TUHV}t[c,n]: \quad c=k+l; \quad t=|k-l|; \quad k=(c+t)/2; \quad l=(c-t)/2 \tag{6}$$

$$\mathrm{TUV/A}[c,n]: \quad c=2k; \quad t=0; \quad \mathrm{A}(c/2,c/2) \tag{7}$$

$$t_{hh}=\frac{|c_{hv}\text{-}t_{hv}|}{2}; \quad c_{hh}=\frac{3c_{hv}+t_{hv}}{2} \tag{8}$$

$$t_{hv}=\frac{|c_{hh}\text{-}3t_{hh}|}{2}; \quad c_{hv}=\frac{c_{hh}+t_{hh}}{2} \tag{9}$$

with *n* remaining indefinite.

In case of tori, each of the above twistings superimpose on the two basic cuttings, thus resulting four classes of twisted tori: (i) H-twist, H-cut HH*t*[*c*,*n*]; (ii) V-twist, H-cut, VH*t*[*c*,*n*]; (iii) H-twist, V-cut, HV*t*[*c*,*n*] and (iv) V-twist, V-cut, VV*t*[*c*,*n*].[36]

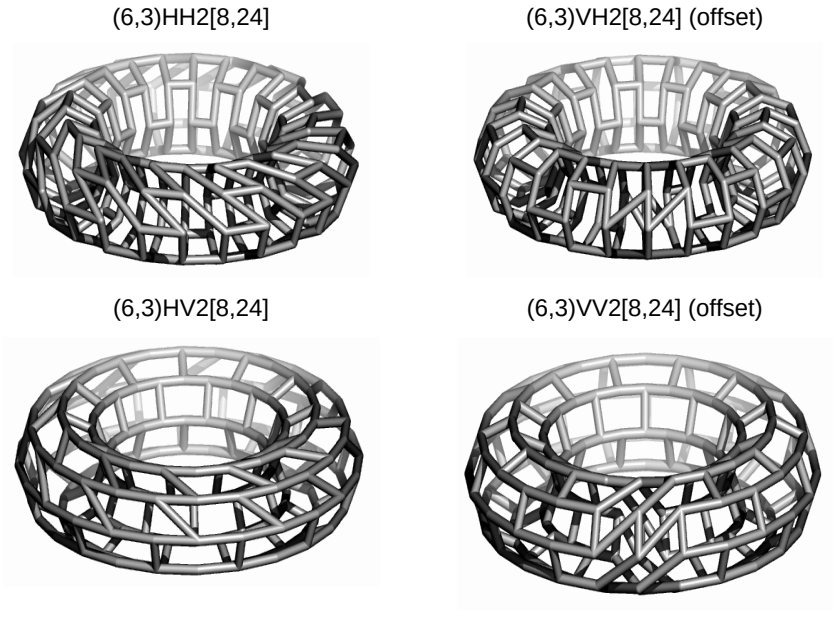

Figure 8. The four classes of twisted polyhex tori (non-optimized geometry).

Figures 9 and 10 illustrate some optimized twisted polyhex tori.

(6,3)HH2[10,100]; N = 1000 (6,3)VH2[10,50]; N = 500

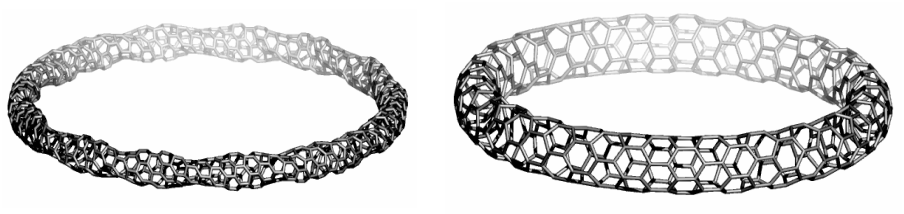

Figure 9. A twisted (6,3) covering in horizontal H-cutting (optimized) toroids.

A toroidal object is drawn as an equivalent planar parallelogram that needs the specification (in two integer parameter notation[22]) of the two involved tubes (Figure 11).

(6,3)VV2[10,100]; N = 1000 (6,3)HV2[10,50]; N = 500

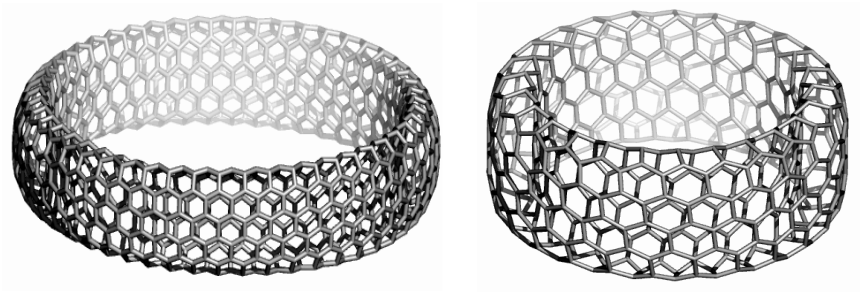

Figure 10. A twisted (6,3) covering in vertical V-cutting (optimized) toroids.

One tube is built up by taking as circumference the rolling-up vector *R*, given in terms of the primitive lattice vectors of graphene:

$$R = ka_1 + la_2 \quad (10)$$

The second tube is formally defined on the translating (or twisting) vector *T*:

$$T = pa_1 + qa_2 \quad (11)$$

Going from a torus, generated as above, to its composing vectors, the first tube can be identified by cutting the object across the tube while the second one results by cutting it around the large hollow. Anyway, a four integer parameter description (*k*,*l*,*p*,*q*) is obtained. Correspondence between the name of tori in our approach X*t*[*c*,*n*] and the four integer parameter (*k*,*l*,*p*,*q*) notation is detailed in Table 1.

The coordinates for the HH4[14,6] torus depicted in Figure 11 are: (5, -4, 3, 3). Note that this representation is not unique and is reducible to three parameter notation, theorized by Kirby *et al*.[12,14]

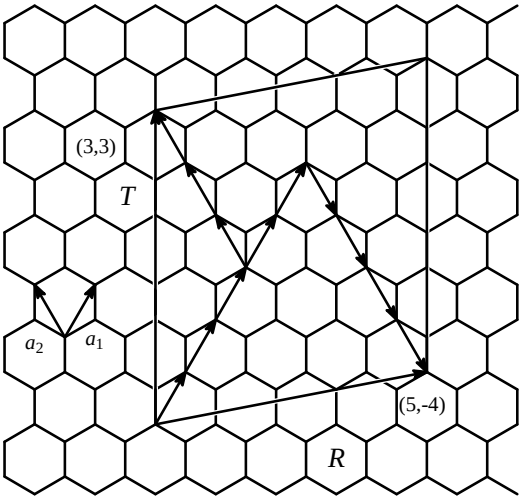

Figure 11. Representation of the torus HH4[14,6] by an equivalent parallelogram involves specification of two tubes: one defined on the rolling-up vector *R* (with integer coordinates (*k*,*l*)) and the other on the translating vector *T* (given by pair (*p*,*q*)). The four parameter specification of the depicted torus is (5, -4, 3, 3).

Table 1

Correspondence between the X*t*[*c*,*n*] and (*k*,*l*,*p*,*q*) notations.

	Torus [*c*,*n*]	Tube *R*	Tube *T*	Torus (*k*,*l*,*p*,*q*)*	*N*
1	H	H/Z	V/A	$(c/2,-c/2,n/2,n/2)$	$2(kq-lp)=cn$
2	V	V/A	H/Z	$(c/2,c/2,n/2,-n/2)$	$2(lp-kq)=cn$
3	HH*t*	HH (tw)	V/A	$[(c-t)/2,-t,n/2,n/2]$	$2(2kq-lp)=cn$
4	HV*t*	HV (tw)	H/Z	$[(c+t)/2,(c-t)/2,n/2,-n/2]$	$2(lp-kq)=cn$
5	VH*t* (offset)	H/Z	HV (tw)	$[c/2,-c/2,(n+t)/2,(n-t)/2]$	$2(kq-lp)=cn$
6	VV*t* (offset)	V/A	HH (tw)	$[c/2,c/2,(n-t)/2,-t)]$	$2(2lp-kq)=cn$

*First pair (*k*,*l*) denotes the rolling-up vector *R* while last pair (*p*,*q*) specifies the translating/twisting vector *T*; (*m*,-*m*) = (*m*,0), is a Z-tube; (*m*,*m*) is an A-tube (see Figure 7).

In our procedure, H-twisting involves an intrinsic chiral (HH or HV) *R*-based tube and a non-twisted *T*-based one (Table 1, entries 3 and 4). Conversely, in V-twisting, the *R*-based tube is a non-chiral (H/Z or V/A) one while the second *T*-based tube is twisted (leading to “offset” closed toroids - Table 1, entries 5 and 6). The resulting

tori are all different, at least as 3D structures, because of distinct embedding. Note that the HV lattice is essentially a HH one, the objects differing, however, as embedding and electronic structure. In generating chiral tori, the above procedure leaves untwisted one of the two constitutive vectors (see above).

We stress that there exist three approchs for generating/naming toroidal lattices non-unique and non-equivalent: Kirby's[11,12], Klein and Zhu[37] and Diudea[26,27]. In this respect several errors have been reported in the literature [38].

Encoding the type of tessellation can be done, for example, by the spiral code.[39-41] It was first proposed for coding and constructing spherical fullerenes. We adapted the spiral code for tubular structures.[42] In a periodic tubular net, the spiral code brings information on size and sequence of faces and embedding the actual object on the parent (4,4)[*c*,*n*] lattice. The α-spiral code for the polyhex tubes is given in Table 2 and for the polyhex toroids is given in Table 3.

Table 2

Ring spiral code of tubes.

	Series	Ring spiral code
1	H/Z[*c*,*n*]	$n \cdot [6^{c/2}]$
2	HHt[*c*,*n*]	$n(1-t/2c)\cdot[6^{c/(1-t/2c))/2}]$
3	HVt[*c*,*n*]	$n/2\cdot[6^{c}]$
4	V/A[*c*,*n*]	$n/2\cdot[6^{c}]$

Table 3

Ring spiral code of tori.

	Series	Ring spiral code
1	H/Z[*c*,*n*]	$[6^{c/2}]^{n}$
2	HH[*c*,*n*]	$[(6^{c/2})^{t}]^{n/t}$
3	HV[*c*,*n*]	$[(6^{c})^{t}]^{n/2t}$
4	VH[*c*,*n*]	$[(6^{n})^{t}]^{c/2t}$
5	VV[*c*,*n*]	$[(6^{n/2})^{t}]^{c/t}$
6	V/A[*c*,*n*]	$[6^{c}]^{n/2}$

The number *t* inside the brackets equals the helicity[43] while the number out the brackets gives the steps of a helix. Note that the helicity could be less than *t*, if an integer number of steps appear.

3. Perfect Clar and Perfect Corannulenic Structures

A perfect Clar structure[44,45] PCS (Figure 12a) is a vertex disjoint set of faces whose boundaries form a 2-factor. A *k*-factor is a regular *k*-valent spanning subgraph. A PCS will include each vertex of *G* once and only once. It is associated

with a Fries structure,[46] which is a Kekulé structure drawn over the maximum possible number of benzenoid (alternating single-double edge) hexagonal faces. A Kekulé structure is a set of pairwise disjoint edges of *G* (covering all its vertices) that coincides with a perfect matching and a 1-factor in Graph Theory.[47] A trivalent polyhedral graph has a PCS if and only if it has a Fries structure.

By extension, a perfect corannulenic system PCorS can be imagined.[36] The operation[48] sequence *Leapfrog-Quadrupling*, applied on trivalent maps, provides a perfect Clar-like corannulenic structure PCorS, with the associated Fries-like structure defined on all the vertices of graph, excepting the corannulenic core ones (Figure 12b, in black).

(a) (6,3)H[24,36] PCS (b) (6,3)H[24,36]) PCorS

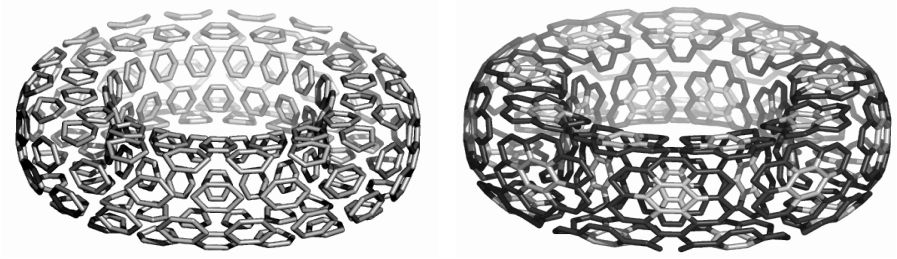

Figure 12. The perfect Clar and Cor structures of a H/Z polyhex torus (see text).

Table 4 gives the criteria for the perfect Clar structures PCS in tori: divisibility by 6 of the net dimensions (see also[49-52]). These criteria superimpose over the metallic (open-shell) character ones. In the opposite, Clar fullerenes (available by Leapfrog operation) show closed-shell structure.[49,50]

The last column in Table 4 gives the criteria for the perfect corannulenic structure PCorS. Any PCorS is necessarily a PCS. The supplementary condition is divisibility by four of the net dimensions.

Table 4

Covering criteria for perfect Clar and perfect Corannulenic structure in polyhex tori originating in square tiled tori

No	Torus	Criterion for perfect Clar structure PCS	Criterion for perfect Corannulenic structure PCorS
	Non-Twisted		
1	H/Z[*c*,*n*]	0 mod (*c*,6)	0 mod (*c*,12); 0 mod (*n*,4)
2	V/A[*c*,*n*]	0 mod (*n*,6)	0 mod (*c*,4); 0 mod (*n*,12)
	H-Twisted		
3	HH*t*[*c*,*n*]	0 mod (*c*,6)	0 mod (*c*,12); 0 mod (*n*,4); 0 mod (*t*,4)

No	Torus	Criterion for perfect Clar structure PCS	Criterion for perfect Corannulenic structure PCorS
4	HV*t*[*c*,*n*]	0 mod (*n*,6) & 0 mod(*t*,6)	0 mod (*c*,4); 0 mod (*n*,12) 0 mod (*t*,12)
	V-Twisted		
5	VH*t*[*c*,*n*]	0 mod (*c*,6) & 0 mod (*t*,6)	0 mod (*c*,12); 0 mod (*n*,4); 0 mod (*t*,12)
6	VV*t*[*c*,*n*]	0 mod (*n*,6)	0 mod (*c*,4); 0 mod (*n*,12); 0 mod (*t*,4)

4. CONCLUSIONS

We have presented a way for modifying the tiling of a nanostructure by cutting the tetragonal (4,4) lattice, embedded in the torus or cylinder, to give the hexagonal (6,3) covering. The topology of polyhex tubes and tori was described by the α-spiral code, adapted for tubular objects.

A perfect corannulenic system PCorS was proposed, by analogy to the well-known perfect Clar system, to give account for some supra-organized fully-resonant π-electronic aromatic systems in fullerenes, nanotubes and nanotori.

It is worthy to note the recent interest in the field of toroidal nanostructures after the publication of results on magnetic behaviour by Terrones *et al* [53]. The authors have shown that corrugated tori, constructed from C_{60} connected along the 3-fold axis, show ring currents of 3 orders of magnitude larger than that of benzene.

REFERENCES

1. B. Grünbaum and G. C. Shephard, *Tilings and Patterns*, Freeman, New York, 1985.
2. D. J. Klein and H. Zhu, in: A. T. Balaban, (Ed.), *From Chemical Topology to Three - Dimensional Geometry*, Plenum Press, New York, 1997, pp. 297-341.
3. B. de La Vaissière, P. W. Fowler, and M. Deza, *J. Chem. Inf. Comput. Sci.*, **2001**, *41*, 376-386.
4. M. Deza, P. W. Fowler, M. Shtorgin, and K. Vietze, *J. Chem. Inf. Comput. Sci.*, **2000**, *40*, 1325-1332.
5. M. Endo, S. Iijima, and M. S. Dresselhaus, *Carbon Nanotubes*, Pergamon, **1996**.
6. P. W. Fowler and D. E. Manolopolous, *An atlas of fullerenes*, Oxford University Press, London, **1994**.
7. M. S. Dresselhaus, G. Dresselhaus, and P. C. Eklund, *Science of fullerenes and carbon nanotubes*, Acad. Press, San Diego, **1996**.
8. K. Tanaka, T. Yamabe, and K. Fukui, *The science and technology of carbon nanotubes*, Elsevier, **1999**.
9. A. T. Balaban, (Ed.), *From Chemical Topology to Three - Dimensional Geometry*, Plenum Press, New York, **1997**.

10. L. Euler, *Novi Comment*. *Acad*. *Sci*. *I*. *Petropolitanae*, **1758**, *4*, 109-160.
11. E. C. Kirby, *Croat*. *Chem*. *Acta*, **1993**, *66*, 13-26.
12. E. C. Kirby, R. B. Mallion, and P. Pollak, *J. Chem*. *Soc*. *Faraday Trans*., **1993**, *89*, 1945-1953.
13. D. J. Klein, *J*. *Chem*. *Inf*. *Comput*. *Sci*., **1994**, *34*, 453-459.
14. E. C. Kirby and P. Pollak, *J*. *Chem*. *Inf*. *Comput*. *Sci*., **1998**, *38*, 66-70.
15. T. Pisanski and J. Shawe-Taylor, *J*. *Chem*. *Inf*. *Comput*. *Sci*., **2000**, *40*, 567-571.
16. A. Graovac, D. Plavšić, M. Kaufman, T. Pisanski, and E. C. Kirby, *J*. *Chem*. *Phys*., **2000**, *113*, 1925-1931.
17. I. Laszlo, A. Rassat, P. W. Fowler, and A. Graovac, *Chem*. *Phys*. *Lett*., **2001**, *342*, 369-374.
18. I. Laszlo and A. Rassat, *J*. *Chem*. *Inf*. *Comput*. *Sci*., **2003**, *43*, 519-524.
19. E. C. Kirby, R. B. Mallion, and P. Pollak, *J*. *Chem*. *Soc*. *Faraday Trans*., **1993**, *89*, 1945- 1953.
20. A. Ceulemans, L. F. Chibotaru, S. A. Bovin, and P. W. Fowler, *J*. *Chem*. *Phys*., **2000**, *112*, 4271-4278.
21. A. L. Ivanovskii, *Russ*. *Chem*. *Rev*.,**1999**, *68*, 103-118.
22. N. Hamada, S. Sawada, and A. Oshiyama, *Phys*. *Rev*. *Lett*., **1992**, *68*, 1579-1581.
23. M. V. Diudea, B. Parv, and O. Ursu, *Torus* 1.1 software program, Babes-Bolyai University, 2001.
24. M. V. Diudea, I. Silaghi-Dumitrescu, and B. Parv, *MATCH*, *Commun*. *Math*. *Comput*. *Chem*., **2001**, *44*, 117-133.
25. M. V. Diudea and E. C. Kirby, *Fullerene Sci*. *Technol*., **2001**, *9*, 445-465.
26. M. V. Diudea, *Bull*. *Chem*. *Soc*. *Japan*, **2002**, *75*, 487-492.
27. M. V. Diudea, B. Parv, and O. Ursu, O., *Studia Univ*. *"Babes-Bolyai"*, **2003,** *48*, 3-10.
28. M. V. Diudea, O. Ursu, and B. Parv, *Studia Univ*. *"Babes-Bolyai"*, **2003,** *48*, 11-20.
29. A. K. Singh, T. M. Briere, V. Kumar, and Y. Kawazoe, *Phys*. *Rev*. *Lett*., **2003**, *91*, 146802-1 - 146802-4.
30. A. K. Singh, V. Kumar, and Y. Kawazoe, *J. Mater*. *Chem*., **2004**, *14*, 555-563.
31. M. V. Diudea, *Fullerenes*, *Nanotubes Carbon Nanostruct*., **2002**, *10*, 273-292.
32. M. V. Diudea, *Phys*. *Chem*. *Chem*. *Phys*., **2002**, *4*, 4740-4746.
33. M. V. Diudea, T. S. Balaban, E. C. Kirby, and A. Graovac, *Phys. Chem*.,*Chem. Phys*., **2003**, *5*, 4210 – 4214.
34. S. L. Fang, A. M. Rao, P. C. Eklund, P. Nikolaev, A. G. Rinzler and R. E. Smalley, *J. Mater*. *Res*., **1998**, *13*, 2405-2411.
35. M. Terrones, H. Terrones, F. Banhart, J-C. Charlier, and P. M. Ajayan, *Science*, **2000**, *288*, 1226-1229.
36. M. V. Diudea, in: M. V. Diudea, Ed., *Nanostructures-Novel Architecture*, NOVA, New York, 2004 (in press).
37. D. J. Klein, H. Zhu, *From Chemical Topology to Three-Dimensional Geometry,* A.T. Balaban Ed., Plenum: New York, **1997**, Chapter 9, 297-341
38. G. Cash, *J*. *Chem*. *Inf*. *Comput*. *Sci*., **1998**, *38*, 58-61
39. D. E. Manolopoulos, J. C. May and S. E. Down, *Chem*. *Phys*. *Lett*., **1991**, *181*, 105-111.
40. G. Brinkmann and P. W. Fowler, *J*. *Chem*. *Inf*. *Comput*. *Sci*., **1998**, *38*, 463-468.
41. P. W. Fowler, T. Pisanski, A. Graovac, and J. Žerovnik, *DIMACS Ser*. *Discrete Maths*. *Theor*. *Comput*. *Sci*., **2000**, *51*, 175-187
42. M. V. Diudea, *Phys*. *Chem., Chem*. *Phys*., **2002**, *4*, 4740-4746
43. D. J. Klein, W. A. Seitz, and T. G. Schmalz, *J*. *Phys*. *Chem*., **1993**, *97*, 1231-1236
44. E. Clar, *Polycyclic Hydrocarbons*, Acad. Press, London, **1964**.
45. E. Clar, *The Aromatic Sextet*, Wiley, New York, **1972**.
46. K. Fries, *J*. *Liebigs Ann*. *Chem*., **1927**, *454*, 121-324.
47. W-Ch. Shiu, P. Ch. B. Lam, and H. Zhang, *Theochem*4, **2000**, p 0210.

48. M. V. Diudea, P. E. John, A. Graovac, M. Primorac, and T. Pisanski, *Croat*. *Chem*. *Acta*, **2003**, *76*, 153-159
49. M. Yoshida, M. Fujita, P. W. Fowler, and E. C. Kirby, *J*. *Chem*. *Soc., Faraday Trans*., **1997**, *93*, 1037-1043
50. P. W. Fowler and T. Pisanski, *J*. *Chem*. *Soc*., *Faraday Trans*., **1994**, *90*, 2865-2871
51. J. R. Dias, *J*. *Chem*. *Inf*. *Comput*. *Sci*., **1999**, *39*, 144-150
52. P. W. Fowler, *Chem*. *Phys*. *Lett*., **1986**, *131*, 444-450
53. J. A. Rodriguez-Manzo, F. Lopez-Urias, M. Terrones and H. Terrones, *Nanolett*, **2004**, *4*, 2179-2183